A DQ Droop Control Strategy for Fixed Frequency VSI-Based AC Microgrids

Mohamed Toub*, Wayne W. Weaver†, Rush D. Robinett III†, Mohamed Maaroufi* and Ghassane Aniba*
*Mohammadia School of Engineering, Mohammed V University of Rabat, Rabat, Morocco
Emails: mohamedtoub@research.emi.ac.ma, {ghassane, maaroufi}@emi.ac.ma
†Michigan Technological University, Houghton, MI, USA
Emails: {wwweaver, rdrobine}@mtu.edu

***Abstract*—The development of distributed energy resources, renewable technologies, and storage systems has given great importance to power electronics that enable coordination and parallel operations of multiple distributed generation units (DGUs) in microgrids. These DGUs are electronically-coupled to each other through power converters that can accurately control their output frequency. This paper presents a droop control technique for fixed frequency VSI-based ac microgrids that combines reference frame transformation, Lyapunov stability analysis, and a modified dc droop control strategy to share active and reactive power between the DGUs without altering the frequency and magnitude of the bus voltage in the islanded microgrid. The simulations show that the proposed distributed droop control ensures proper sharing of the active and reactive power, and regulates the bus voltage at the nominal value while operating at a fixed frequency.**

***Index Terms*—Active and reactive power-sharing, droop control, microgrids, reference frame transformation.**

I. Introduction

THE electricity grid of the future can be seen as the interconnection of multiple microgrids. These microgrids can be either connected to the grid or operated autonomously. In the grid-tied mode, the microgrid voltage magnitude and frequency are dictated and maintained by the main grid, and the distributed generation units (DGUs) are only responsible for controlling the injected power. The islanded mode is more challenging than the grid-tied mode since the DGUs should coordinate with each other to balance the load and regulate the voltage magnitude and frequency of the microgrid.

Different control schemes have been proposed in the literature for coordination and load sharing between parallel-connected DGUs in islanded microgrids. These methods are divided into two main categories. The first category covers the active load sharing techniques that ensure accurate load sharing and voltage regulation. These techniques include the centralized [1], the master-slave method [2], and the average load sharing scheme [3]. However, they pose the risk of a single point of failure as they depend on communication technology for measurements and information exchange between the DGUs. The second category covers the communication free schemes, mainly the droop characteristic methods, that use only local measurements to share the load and maintain the voltage [4].

Droop control in ac microgrids tries to mimic the conventional electrical grid behavior. It exploits the relationships between real power and frequency $P-f$ and between reactive power and voltage magnitude $Q-V$, that govern the spinning machines of synchronous generators, to share both active and reactive power between the generators. This conventional droop control adjusts the DGUs frequency and voltage magnitude references in response to an active or reactive power change [5]

To achieve active and reactive power-sharing without changing the microgrid frequency, angle droop control has been proposed in [6]. This technique depends on accurate voltage angle measurement relative to a reference angle. It also requires large values of angle droop gains to ensure proper sharing of the load, which may lead to instability of the overall system. To overcome these issues, authors in [7] use a supplementary angle droop control loop that improves the stability even with the high angle droop gains. However, the design of the additional loop appears to be complicated.

In [8], the authors present a current magnitude droop control strategy for voltage source inverters (VSIs) in current control mode. This strategy combines linear current regulator and predictive voltage control to share the load and regulate the voltage level. However, this method is designed for single-phase systems and can only achieve equal load sharing.

In this work, a novel droop control scheme for DGUs in fixed frequency VSI-based ac microgrids is presented. One particular idea behind this method is to exploit the inherent property of VSIs to tightly control their output waveform in order to operate the microgrid at a fixed frequency. The other idea is to transform a balanced three-phase ac system into two coupled dc systems using the dq0 transformation. Hence, dc droop control with integral feedback can be applied to each of the two resulting dq systems to separately share the d and q-axis components of the load current. Consequently, the active and reactive power are shared without deviation of the bus voltage. A droop stability analysis is performed to prove that the cross-coupling terms in the two equivalent dc systems do not affect the stability of the system with droop control. A two DGUs microgrid is simulated to demonstrate the efficacy of the proposed droop technique regarding sharing active and reactive power and maintaining the bus voltage at its nominal value even when the load changes.

II. Microgrid Model

For simplicity, the two parallel-connected DGUs microgrid model presented in [9] will be used for the simulation of the proposed droop control. Nevertheless, this strategy can be applied to a microgrid with N parallel-connected DGUs. The studied microgrid consists of 1) two DGUs composed each of a VSI connecting a dc voltage source to the ac bus through a series (R_{li}, L_{li}) line/filter. 2) A parallel three-phase (RC) network representing the ac load connected to the bus.

The state equations of the ith DGU ($i = 1, 2$) in the abc-frame are obtained from its line/filter dynamics as

$$L_{li}\dot{\boldsymbol{I}}_{\boldsymbol{abci}} = -R_{li}\boldsymbol{I}_{\boldsymbol{abci}} + \boldsymbol{V}_{\boldsymbol{abci}} - \boldsymbol{V}_{\boldsymbol{B}} \quad (1)$$

This work is supported in part by the US National Science Foundation (Grant #1541148), the Richard and Elizabeth Henes Professorship of Mechanical Engineering at Michigan Technological University, and the Institute for Research on Solar and new Energies (IRESEN) in Morocco (reference: InnoTherm-13-MicroCSP).

978-1-5386-2251-3/18/$31.00 ©2018 IEEE

where $\boldsymbol{V_B}$, $\boldsymbol{V_{abci}}$, and $\boldsymbol{I_{abci}}$ are the three-phase ac quantities vectors of the bus voltage, the output voltage of the ith DGU's VSI ($i = 1, 2$) and its corresponding line/filter current, respectively.

For the RC load, the state equations in the abc-frame are

$$C_B\dot{\boldsymbol{V}}_{\boldsymbol{B}} = -\frac{\boldsymbol{V_B}}{R_B} + \boldsymbol{I_{abc1}} + \boldsymbol{I_{abc2}} \tag{2}$$

Assuming balanced three-phase ac system, the dq0 transformation is applied to the state equations (1) and (2) in the stationary abc-frame, to obtain the state equations of the VSI-based microgrid with two DGUs connected to a common bus, in the dq-frame rotating at a constant speed ω proportional to the microgrid frequency [9]:

$$L_{l1}\dot{I}_{d1} = -R_{l1}I_{d1} + V_{d1} - V_{dB} + \omega L_{l1}I_{q1} \tag{3a}$$
$$L_{l2}\dot{I}_{d2} = -R_{l2}I_{d2} + V_{d2} - V_{dB} + \omega L_{l2}I_{q2} \tag{3b}$$
$$C_B\dot{V}_{dB} = -\frac{V_{dB}}{R_B} + I_{d1} + I_{d2} + \omega C_B V_{qB} \tag{3c}$$
$$L_{l1}\dot{I}_{q1} = -R_{l1}I_{q1} + V_{q1} - V_{qB} - \omega L_{l1}I_{d1} \tag{3d}$$
$$L_{l2}\dot{I}_{q2} = -R_{l2}I_{q2} + V_{q2} - V_{qB} - \omega L_{l2}I_{d2} \tag{3e}$$
$$C_B\dot{V}_{qB} = -\frac{V_{qB}}{R_B} + I_{q1} + I_{q2} - \omega C_B V_{dB}, \tag{3f}$$

with V_{dB}, V_{qB}, V_{di}, V_{qi}, I_{di}, and I_{qi} are the direct and quadrature components of the bus voltage, the VSI's output voltage of the ith DGU ($i = 1, 2$) and the corresponding line/filter current, respectively.

III. DQ Current Droop Control

To share the total injected active power, P_T, and reactive power, Q_T, between parallel-connected DGUs, one only needs to share the dq components of the load current. Indeed, let γ_1 be the share of the first DGU and $\gamma_2 = 1 - \gamma_1$ the share of the second DGU such that

$$I_{di} = \gamma_i I_{dB} \tag{4a}$$
$$I_{qi} = \gamma_i I_{qB}. \tag{4b}$$

The active power supplied by the ith DGU is

$$\begin{aligned} P_i &= V_{dB}I_{di} + V_{qB}I_{qi} \\ &= \gamma_i(V_{dB}I_{dB} + V_{qB}I_{qB}) \\ &= \gamma_i P_T. \end{aligned} \tag{5}$$

Likewise, the reactive power supplied by the ith DGU is

$$\begin{aligned} Q_i &= V_{qB}I_{di} - V_{dB}I_{qi} \\ &= \gamma_i Q_T. \end{aligned} \tag{6}$$

The three-phase ac side of the system can be seen as two equivalent dc systems as shown in Fig. 1. Although the two systems are cross-coupled, the dc droop control can still be applied to the d and q-axis circuits, separately. The droop control in dc systems is realized by simply implementing a virtual resistive impedance to share the load current according to the droop settings [10]. From a control point of view, this is equivalent to using a proportional controller that sets the current references proportionally to the error between the bus voltage and the droop voltage setting. However, the intrinsic steady-state error of proportional controllers translates to a voltage deviation that makes the bus voltage magnitude load-dependent. To cope with this issue, this paper modifies the dc droop control by adding a virtual inductance, parallel to the virtual resistance, which introduces an integral term to cancel the steady-state error and regulate the voltage magnitude at its nominal value.

Fig. 2 shows the equivalent terminal characteristics of the ith DGU with droop control in dq-frame. The dq-components of the reference for the current injected by the ith DGU ($i = 1, 2$) into the bus are set by the droop controller as

$$I^*_{di} = \frac{V_{Dd} - V_{dB}}{R_{D,i}} + \frac{\int(\hat{V}_{dB} - V_{dB})dt}{L_{D,i}} \tag{7a}$$
$$I^*_{qi} = \frac{V_{Dq} - V_{qB}}{R_{D,i}} + \frac{\int(\hat{V}_{qB} - V_{qB})dt}{L_{D,i}} \tag{7b}$$

where $R_{D,i}$ is the droop virtual resistance, $L_{D,i}$ is the droop virtual inductance, V_{Dd} and V_{Dq} are the droop voltage settings in dq coordinates, and $\hat{V}_{dB}$, $\hat{V}_{qB}$, $\hat{I}_{dB}$ and $\hat{I}_{qB}$ are the dq-components of the nominal bus voltage and the nominal load current, respectively.

A. Droop stability analysis

Assuming that the DGUs can track the current set points dictated by the droop controller through the fast inner current loop, the dynamics of the line/filters' current error can be neglected, and the injected bus currents in (3a) and (3b) are substituted by the right-hand sides of (7) giving

$$C_B\dot{V}_{dB} = \frac{-V_{dB}}{R_B} + \frac{V_{Dd} - V_{dB}}{R_D} + \frac{\int(\hat{V}_{dB} - V_{dB})dt}{L_D} + \omega C_B V_{qB} \tag{8a}$$
$$C_B\dot{V}_{qB} = -\frac{V_{qB}}{R_B} + \frac{V_{Dq} - V_{qB}}{R_D} + \frac{\int(\hat{V}_{qB} - V_{qB})dt}{L_D} - \omega C_B V_{dB} \tag{8b}$$

where $1/R_D = (1/R_{D,1} + 1/R_{D,2})$ and $1/L_D = (1/L_{D,1} + 1/L_{D,2})$.

Let e_d and e_q be the dq bus voltage errors defined by

$$e_d = \hat{V}_{dB} - V_{dB} \tag{9a}$$
$$e_q = \hat{V}_{qB} - V_{qB}. \tag{9b}$$

From (8) and (9), the state space equation of the system with droop control is

$$\boldsymbol{E_i}\dot{\boldsymbol{x}} = \boldsymbol{A_i}\boldsymbol{x} \tag{10}$$

with $\boldsymbol{x} = \left[e_d,\ e_q,\ \int e_d dt,\ \int e_q dt\right]^T$ is the state vector. The matrices in (10) are given by

$$\boldsymbol{E_i} = \begin{bmatrix} C_B & 0 & 0 & 0 \\ 0 & C_B & 0 & 0 \\ 0 & 0 & \frac{1}{L_D} & 0 \\ 0 & 0 & 0 & \frac{1}{L_D} \end{bmatrix} \tag{11}$$

$$\boldsymbol{A_i} = \begin{bmatrix} \frac{-1}{R_B} + \frac{-1}{R_D} & \omega C_B & \frac{-1}{L_D} & 0 \\ -\omega C_B & \frac{-1}{R_B} + \frac{-1}{R_D} & 0 & \frac{-1}{L_D} \\ \frac{1}{L_D} & 0 & 0 & 0 \\ 0 & \frac{1}{L_D} & 0 & 0 \end{bmatrix}. \tag{12}$$

The stability analysis is performed using the Lyapunov second method by choosing the Lyapunov function candidate as the Hamiltonian $\mathcal{H}_i$ of the system with droop control [11]:

$$\mathcal{H}_i(\boldsymbol{x}) = \frac{1}{2}\boldsymbol{x}^T\boldsymbol{E_i}\boldsymbol{x} > 0. \tag{13}$$

$\mathcal{H}_i$ is positive definite and qualifies as a Lyapunov function. The time derivative of the Hamiltonian is

$$\begin{aligned} \dot{\mathcal{H}}_i(\boldsymbol{x}) &= \boldsymbol{x}^T\boldsymbol{E_i}\dot{\boldsymbol{x}} \\ &= \boldsymbol{x}^T\boldsymbol{A_i}\boldsymbol{x} \\ &= -\left(\frac{1}{R_B} + \frac{1}{R_D}\right)\left(e_d^2 + e_q^2\right) \le 0. \end{aligned} \tag{14}$$

It should be mentioned that $\boldsymbol{A_i}$ is the sum of a diagonal matrix and a skew-symmetric matrix with the cross-coupling terms in the off-diagonal entries. Consequently, these cross-coupling terms have canceled each other out in (14).

A sufficient condition for asymptotic stability is $\dot{\mathcal{H}}_i(\boldsymbol{x}) < 0$, for all $\boldsymbol{x} \neq 0$. However, the time derivative of the Hamiltonian is negative semidefinite since it does not depend on the integrators' dynamics. Indeed, $\dot{\mathcal{H}}_i(\boldsymbol{x}) = 0$ for $e_d = e_q = 0$, irrespective to the values of $\int e_d dt$ and $\int e_q dt$. Hence, to prove asymptotic stability, the higher order derivatives of the Hamiltonian are investigated [12].

Let Ω be a non-empty set such that $\boldsymbol{x} \in \Omega$ implies $\dot{\mathcal{H}}(\boldsymbol{x}) = 0$. According to (14), $\Omega = \{\boldsymbol{x} | e_d = e_q = 0\}$.

Then, the first order time derivate of the Hamiltonian

$$\dot{\mathcal{H}}_i(\boldsymbol{x}) \quad = \quad 0 \quad \forall \boldsymbol{x} \in \Omega. \tag{15}$$

The second order time derivate of the Hamiltonian is

$$\begin{aligned}
\ddot{\mathcal{H}}_i(\boldsymbol{x}) &= 2\boldsymbol{x}^T \boldsymbol{A_i} \dot{\boldsymbol{x}} && (16)\\
&= \frac{2}{C_B}\left(\frac{1}{R_B}+\frac{1}{R_D}\right)\left[\left(\frac{1}{R_B}+\frac{1}{R_D}\right)\left(e_d^2+e_q^2\right)\right.\\
&\quad \left.+\frac{1}{L_D}\left(e_d\int e_d dt + e_q \int e_q dt\right)\right]\\
&= \frac{2}{C_B}\left(\frac{1}{R_B}+\frac{1}{R_D}\right)\left[-\dot{\mathcal{H}}_i(\boldsymbol{x})\right.\\
&\quad \left.+\frac{1}{L_D}\left(e_d\int e_d dt + e_q \int e_q dt\right)\right]\\
&= 0 \quad \forall \boldsymbol{x} \in \Omega. && (17)
\end{aligned}$$

The third order time derivative of the Hamiltonian is

$$\begin{aligned}
\dddot{\mathcal{H}}_i(\boldsymbol{x}) &= \frac{2}{C_B}\left(\frac{1}{R_B}+\frac{1}{R_D}\right)\left[-\ddot{\mathcal{H}}_i(\boldsymbol{x})+\frac{1}{L_D}\left(e_d^2\right.\right.\\
&\quad \left.\left.+e_q^2+\dot{e}_d\int e_d dt+\dot{e}_q\int e_q dt\right)\right]\\
&= \frac{2}{C_B}\left(\frac{1}{R_B}+\frac{1}{R_D}\right)\left[-\ddot{\mathcal{H}}_i(\boldsymbol{x})+\frac{1}{C_B L_D}\left[e_d^2\right.\right.\\
&\quad +e_q^2-\left(\frac{1}{R_B}+\frac{1}{R_D}\right)\left(e_d\int e_d dt+e_q\int e_q dt\right)\\
&\quad +\omega C_B\left(e_q\int e_d dt - e_d\int e_q dt\right)\\
&\quad \left.\left.-\frac{1}{L_D}\left(\left(\int e_d dt\right)^2+\left(\int e_q dt\right)^2\right)\right]\right], && (18)
\end{aligned}$$

then, for $\boldsymbol{x} \in \Omega$

$$\begin{aligned}
\dddot{\mathcal{H}}_i(\boldsymbol{x}) &= -\frac{2}{\left(C_B L_D\right)^2}\left(\frac{1}{R_B}+\frac{1}{R_D}\right)\left[\left(\int e_d dt\right)^2\right.\\
&\quad \left.+\left(\int e_q dt\right)^2\right]. && (19)
\end{aligned}$$

Hence,

$$\dddot{\mathcal{H}}_i(\boldsymbol{x}) \quad < \quad 0 \quad \forall \boldsymbol{x} \in \Omega. \tag{20}$$

The order of the first non-zero time derivative of the Hamiltonian $\mathcal{H}_i$ is an odd number. Therefore, according to [12, Theorem 8.5 on p. 363], the system with droop control is asymptotically stable.

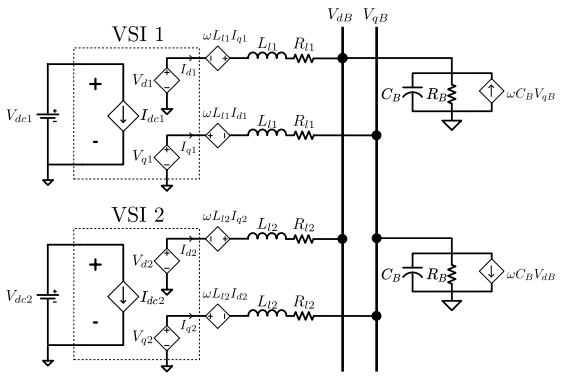

Fig. 1. Two DGUs and RC load connected to a common bus in dq-frame.

B. Droop control settings

To guarantee precise sharing of the load current/power between the DGUs, the droop virtual resistances and inductances should verify

$$\gamma_1 R_{D,1} = \gamma_2 R_{D,2} \tag{21a}$$

$$\gamma_1 L_{D,1} = \gamma_2 L_{D,2}. \tag{21b}$$

These droop resistances and inductances should be tunned carefully since they also affect the injected current/power transient.

The droop voltage settings, V_{Dd} and V_{Dq}, are chosen to maintain the desired nominal bus voltage values. According to (3), in nominal steady-state, the dq components of the nominal load current are

$$\hat{I}_{dB} = \hat{I}_{d1} + \hat{I}_{d2} = \frac{\hat{V}_{dB}}{R_B} - \omega C_B \hat{V}_{qB} \tag{22a}$$

$$\hat{I}_{qB} = \hat{I}_{q1} + \hat{I}_{q2} = \frac{\hat{V}_{qB}}{R_B} + \omega C_B \hat{V}_{dB}. \tag{22b}$$

Hence, the dq components of the load current in (4) can by replaced by the right-hand sides of (22), while the left-hand sides of (4) are replaced by the right-hand sides of (7) after substituting the dq-components of the bus voltage by their nominal values:

$$\frac{V_{Dd} - \hat{V}_{dB}}{R_{D,i}} = \gamma_i \left(\frac{\hat{V}_{dB}}{R_B} - \omega C_B \hat{V}_{qB}\right) \tag{23a}$$

$$\frac{V_{Dq} - \hat{V}_{qB}}{R_{D,i}} = \gamma_i \left(\frac{\hat{V}_{qB}}{R_B} + \omega C_B \hat{V}_{dB}\right). \tag{23b}$$

Then, the droop voltage settings are

$$V_{Dd} = \left(1 + \frac{\gamma_i R_{D,i}}{R_B}\right)\hat{V}_{dB} - \gamma_i R_{D,i} \omega C_B \hat{V}_{qB} \tag{24a}$$

$$V_{Dq} = \left(1 + \frac{\gamma_i R_{D,i}}{R_B}\right)\hat{V}_{qB} + \gamma_i R_{D,i} \omega C_B \hat{V}_{dB}. \tag{24b}$$

IV. Simulation Results

The system of Fig. 1 was modeled and simulated in Wolfram SystemModeler using the Modelica modeling language [13]. The two VSIs are operated at a 60 Hz fixed frequency, and the shares of the DGUs are set such that $\gamma_1 = 0.6$ and $\gamma_2 = 0.4$. The system is allowed to reach a steady-state before stepping down the load resistance R_B and the load capacitance C_B to 10 Ω and 50 μF, respectively, at $t = 0.08$ s.

Fig. 3 shows that, under nominal conditions, the amplitude of three-phase bus voltage is regulated at the 200 V nominal value. After the load change, the bus voltage exhibits a small and brief transient

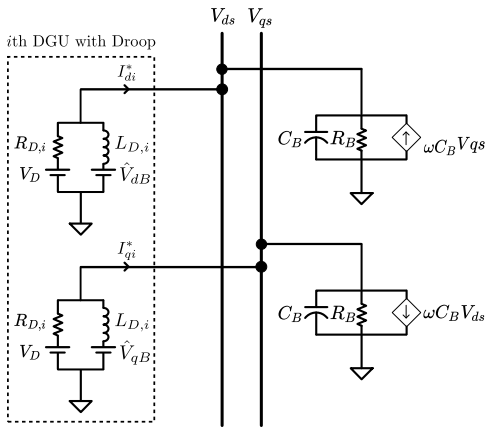

Fig. 2. Equivalent characteristics of a DGU with droop control in dq-frame.

response before it returns to its nominal value. This transient response can be clearly seen for the direct and quadrature components of the bus voltage. Hence, it can be concluded that the proposed droop control method can maintain stable operation of the microgrid without voltage deviation after the load change.

From Fig. 4, it can be seen that the nominal active power absorbed by the RC load is $P_T = 3$ kW while the active power injected by DGU 1 and DGU 2 are $P_1 = 1.8$ kW $= 0.6 \times P_T$ and $P_2 = 1.2$ kW $= 0.4 \times P_T$, respectively. Furthermore, the two DGUs respond to the load step change by proportionally increasing their injected power to $P_1' = 3.6$ kW and $P_2' = 2.4$ kW which represents, respectively, 60% and 40% of the new total load $P_T' = 6$ kW. These results reveal that the proposed droop control is able to accurately share active power between the three DGUs according to the predefined proportions. Fig. 4 also shows that the proposed droop control was able to proportionally share the reactive power, as well, between the DGUs. The first DGU supplies 60% of the total reactive power absorbed by the loads ($Q_T \approx -2.25$ kVar), whereas the second DGU provides the remaining 40%. Moreover, the DGUs respond to the load step changes by adjusting the DGUs' supplied reactive power proportionally.

V. Conclusion

This paper presented a decentralized droop method that shares the active and reactive power demand between parallel-connected DGUs and regulates the bus voltage using only local measurements without further communication infrastructure. It is shown that the d and q-axis equivalent systems can be controlled independently to droop the d and q-axis components of the current proportionally to the d and q-axis bus voltages, respectively. Simulation results demonstrate the ability of the proposed droop method to proportionally adjust the DGUs injected powers following a load change and to maintain the load voltage regulated at the nominal value. Furthermore, the proposed droop method was able to operate without frequency change which makes it suitable for fixed-frequency VSI-based ac microgrids.

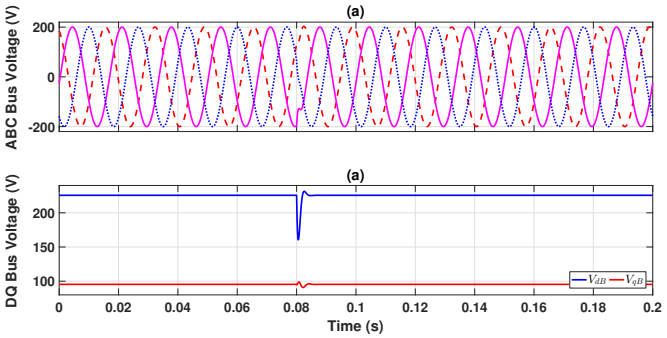

Fig. 3. a) ABC and b) DQ bus voltage response with the load resistance and capacitance stepped down to 10 Ω and 50 μF, respectively, at $t = 0.08$ s.

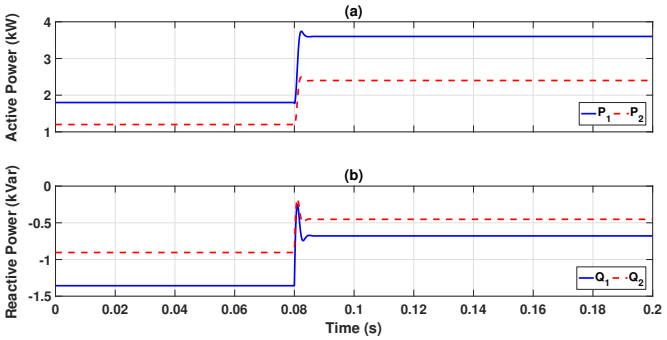

Fig. 4. a) Active and b) reactive power response with the load resistance and capacitance stepped down to 10 Ω and 50 μF, respectively, at $t = 0.08$ s.

References

[1] N. L. Daz, A. C. Luna, J. C. Vasquez, and J. M. Guerrero, "Centralized control architecture for coordination of distributed renewable generation and energy storage in islanded ac microgrids," *IEEE Transactions on Power Electronics*, vol. 32, no. 7, pp. 5202–5213, July 2017.

[2] D. I. Brandao, T. Caldognetto, F. P. Marafo, M. G. Simes, J. A. Pomilio, and P. Tenti, "Centralized control of distributed single-phase inverters arbitrarily connected to three-phase four-wire microgrids," *IEEE Transactions on Smart Grid*, vol. 8, no. 1, pp. 437–446, Jan 2017.

[3] H. Nazaripouya, H. Mokhtari, and E. Amiri, "Using optimal controller to parallel three-phase 4-leg inverters with unbalance loads," in *IEEE Int. Conf. on Power Electronics, Intelligent Control and Energy Systems (ICPEICES)*. IEEE, 2016, pp. 1–6.

[4] M. C. Chandorkar, D. M. Divan, and R. Adapa, "Control of parallel connected inverters in standalone AC supply systems," *IEEE Trans. Ind. Appl.*, vol. 29, no. 1, pp. 136–143, Jan. 1993.

[5] X. Hou, Y. Sun, W. Yuan, H. Han, C. Zhong, and J. M. Guerrero, "Conventional P–ω/Q–V droop control in highly resistive line of low-voltage converter-based ac microgrid," *Energies*, vol. 9, no. 11, p. 943, Nov. 2016.

[6] R. Majumder, G. Ledwich, A. Ghosh, S. Chakrabarti, and F. Zare, "Droop control of converter-interfaced microsources in rural distributed generation," *IEEE Trans. Power Del.*, vol. 25, no. 4, pp. 2768–2778, Oct. 2010.

[7] R. Majumder, B. Chaudhuri, A. Ghosh, R. Majumder, G. Ledwich, and F. Zare, "Improvement of stability and load sharing in an autonomous microgrid using supplementary droop control loop," *IEEE Trans. Power Syst.*, vol. 25, no. 2, pp. 796–808, May 2010.

[8] B. Shoeiby, R. Davoodnezhad, D. G. Holmes, and B. P. McGrath, "A new current control droop strategy for vsi-based islanded microgrids," in *2014 International Power Electronics Conference (IPEC-Hiroshima 2014 - ECCE ASIA)*, May 2014, pp. 1482–1489.

[9] T. Hassell, W. W. Weaver, R. D. Robinett, D. G. Wilson, and G. G. Parker, "Modeling of inverter based AC microgrids for control development," in *IEEE Conf. Control Applications (CCA)*, 2015, pp. 1347–1353.

[10] W. W. Weaver, R. D. Robinett, G. G. Parker, and D. G. Wilson, "Energy storage requirements of dc microgrids with high penetration renewables under droop control," *International Journal of Electrical Power & Energy Systems*, vol. 68, pp. 203–209, Jun. 2015.

[11] R. D. Robinett III and D. G. Wilson, *Nonlinear power flow control design: utilizing exergy, entropy, static and dynamic stability, and Lyapunov analysis*. Springer Science & Business Media, 2011.

[12] H. Schaub and J. L. Junkins, *Analytical Mechanics of Space Systems*, 2nd ed. Reston, VA: AIAA Education Series, 2009.

[13] Wolfram Research, Inc., "Wolfman SystemModeler 4.2," 2015. [Online]. Available: https://www.wolfram.com/system-modeler/